

# From Regions to Stacks: Spatial and Temporal Downscaling of Power Pollution Scenarios

Benjamin F. Hobbs, *Fellow, IEEE*, Ming-Che Hu, Yihsu Chen, *Member, IEEE*, J. Hugh Ellis, Anthony Paul, Dallas Burtraw, and Karen L. Palmer

**Abstract**—National energy models produce aggregate scenarios of generation capacity, energy output, and emissions. However, we need finer scales to study the impact of resource use and air pollution because timing and location determine impacts on sensitive ecosystems and human populations.

We present a framework for disaggregating emissions projections to a scale compatible with air quality simulation models. The framework comprises three models that site new power plants consistent with historical patterns while recognizing water, transmission, fuel, and other factors that constrain siting, and then dispatches them consistent with those constraints. The resulting hourly emissions from individual plants are consistent with meteorology, in that peak demands and emissions occur during those hours when temperatures associated with such demands occur. Further, annual emissions vary in a way consistent with year-to-year changes in weather.

An application of the framework disaggregates 2030 NO<sub>x</sub> emissions from a national electricity model in an eight-state region under two climate scenarios: no climate change (“1990s”) and accelerated change (“2050s”). Between-year variations in emissions patterns under a particular climate exceed differences between average patterns of the two scenarios. This is in part because NO<sub>x</sub> emissions are capped; thus, the total cannot change, only its distribution over time and space.

**Index Terms**—Air pollution, climate change, dispatch, environment, generation expansion, Haiku, power plant siting.

## I. INTRODUCTION

LONG run models of power sector investment and operations are widely used to project how the power sector could evolve in response to changes in technology, policy, climate, and economic conditions. Notable are the IPM [29] and Haiku [21] power models and the electricity module of NEMS [27]. Users are interested in how different assumptions affect the mix and cost of generation; market prices; resource use, such

Manuscript received January 13, 2009; revised June 24, 2009. First published January 29, 2010; current version published April 21, 2010. This work was supported by USEPA STAR Grants R929731010 and RD83183601 and by NSF Grant ECS 0621920. Any opinions or errors are solely the authors’ responsibility, and do not necessarily represent the position of the sponsor. Paper no. TPWRS-01041-2008.

B. F. Hobbs and J. H. Ellis are with The Johns Hopkins University, Baltimore, MD 21218 USA (e-mail: bhobbs@jhu.edu; hugh.ellis@jhu.edu).

M.-C. Hu is with the University of Illinois, Urbana, IL 61801 USA (e-mail: mchu@illinois.edu).

Y. Chen is with the University of California, Merced, CA 95343 USA (e-mail: yihsu.chen@ucmerced.edu).

A. Paul, D. Burtraw, and K. L. Palmer are with Resources for the Future, Washington, DC 20036 USA (e-mail: paul@rff.org; burtraw@rff.org; palmer@rff.org).

Color versions of one or more of the figures in this paper are available online at <http://ieeexplore.ieee.org>.

Digital Object Identifier 10.1109/TPWRS.2009.2036801

as water, fuel, or land; and impacts of so-called “conventional” pollutants (particulates, SO<sub>2</sub>, NO<sub>x</sub>) and greenhouse gasses.

As an example of such analyses, it has been predicted that climate warming would increase electricity use [e.g., [1], [10]], decrease hydropower availability, and increase thermal generation and associated emissions [26], [31]. For instance, we have estimated short run sensitivities of summer electricity demand to temperature (on the order of 4%/°C for the mid-Atlantic region) [5]; long run sensitivities are even greater, as climate warming would increase investment in air conditioning. Even if legislation caps annual emissions (as in the case of SO<sub>2</sub> and NO<sub>x</sub> in much of the U.S.), their impacts could change. In particular, shifts in emissions timing (more during summer, coinciding with weather conducive to ozone episodes) and location, together with changed meteorology, could significantly affect tropospheric ozone levels and their health impacts [2], [16], [18].

However, with the exception of greenhouse gases, the impact of a ton of pollution or the consumption of a unit of water depends on *where* and *when* those emissions and consumption take place. For instance, air pollution is transported downwind, and is subject to complex transformations that are time and space dependent. (For example, although NO<sub>x</sub> emissions usually enhance tropospheric ozone formation, under some conditions NO<sub>x</sub> can instead be inhibiting [e.g., [32]].) Further, the health effects of the resulting ambient concentrations of pollution depend on population location, activity, and susceptibility. For example, a national model may project  $X$  MW of coal-fired plant in PJM, but its health impact depends on whether emissions take place close to population concentrations on the eastern seaboard or further upwind in the midwest [e.g., [17]]. Thus, full understanding of the effects of a power sector scenario requires site- and hour-specific emissions projections.

This requirement does not imply that *accurate* forecasts are needed. Rather, emissions from alternative climate, policy, economic, and technology scenarios need to be downscaled in a consistent, logical, and convenient way so that possible impacts can be explored using air quality models. No particular scenario should be taken as a precise prediction; rather, the goal is insight about trends and potential effects.

Our purpose here is to present a modeling framework for creating geographically and temporally disaggregated emissions scenarios for the power sector on a multidecadal time-scale for use with air quality models such as Models-3 CMAQ [28]. The intent is to provide a theoretically defensible, transparent, and practical method for downscaling emissions from national energy models such as IPM, Haiku, and NEMS.

The framework uses a sequence of models representing market-driven electricity supply and facility location con-

strained by land use and policy-based emissions limits. First, a national electricity model (here, Haiku [21]) is used to solve for regional technology, demand, and emissions totals for each of several multistate regions in the U.S. Then in the downscaling step, a series of three finer-scaled regional models allocate specific generation facilities to the county level and simulate their operation for specific hourly sequences of weather consistent with assumed climate scenarios, using the regional technology, energy, and emissions totals as boundary conditions. A similar but simpler two-step approach has been used for environmental analysis of national energy policies since the 1970s National Coal Utilization Assessment [e.g., [3]], which assessed the local air pollution and other impacts of greater coal use. That study used plant siting models (such as [20] for the northeastern U.S.) to disaggregate results of national energy scenarios. However, unlike our study, it did not consider transmission constraints in a realistic fashion, nor did it produce hourly emissions that are consistent with how loads vary with weather.

Of course, the amounts, locations, and timing of power sector emissions are sensitive to economic and technological assumptions. This has two implications. First, a transparent, theoretically defensible, and flexible method is needed to create emissions scenarios. Transparency results from a logical and readily understood connection between assumptions and results. Theoretical defensibility means that the methodology provides a coherent and acceptable framework for representing the market and policy drivers of power plant location and operation. Flexibility is required so that the implications of alternative assumptions can be readily explored. Consistent with the worldwide trend towards liberalization of power markets, we use the concept of a competitive market equilibrium, constrained by emissions policy and siting restrictions, as the organizing principle for spatially and temporally disaggregating power sector emissions. This paradigm is consistent with frameworks used by most national electric power sector models [e.g., [29]].

Our downscaling framework is a generalization of early linear programming-based regional power plant siting methods developed to spatially disaggregate emissions [e.g., [6], [7], [20], reviewed in [11]]. Our models assume that producers behave competitively and minimize the cost of the investments and dispatch needed to meet demand. The framework attempts to provide more realistic projects of emissions patterns than previous regional emissions allocation methods by adding the following features that the earlier generation of models lack:

- Unlike transshipment or transportation load flow formulations of previous downscaling methods, we represent the power grid as a linearized dc load flow with losses [24].
- New power plants are allocated to counties within a subregion consistent with siting probabilities estimated using statistical models that relate past siting decisions to county-specific factors. Furthermore, the amounts of capacity added are multiples of typical unit sizes, avoiding the unrealistically small plants that some previous downscaling methods yielded (e.g., nuclear facilities of 10 MW) [11].
- Hourly load profiles are produced that are consistent with hourly meteorology, in the sense that weather conditions that are known to produce higher loads (hot weather in

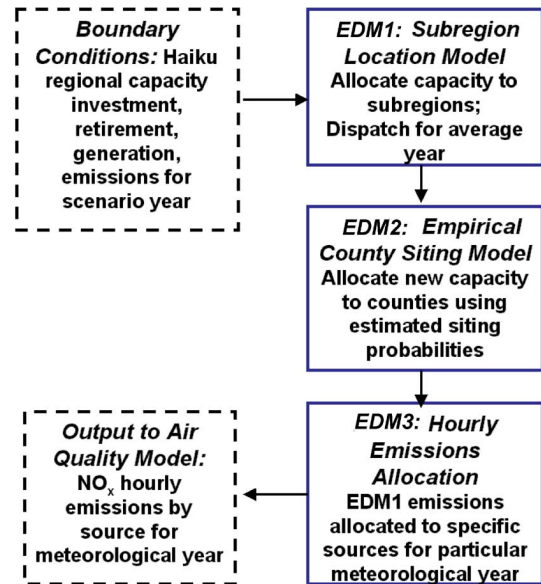


Fig. 1. Flow chart for downscaling framework.

the summer) actually yield greater demands and emissions. This is important because such conditions favor ozone formation.

Other recent downscaling models have some but not all of these features; for instance, [31] includes load flow constraints when projecting emissions in the Western U.S. under climate change.

The organization of the paper is as follows. In Section II, we briefly summarize the downscaling framework, as well as the national energy model we use in the application (Haiku). Section III presents the formulations of the three models that make up the framework. Section IV provides illustrative downscaling results for a case study: 2030 demand and supply conditions in an eight state region in the eastern U.S. under two alternative climate scenarios. We offer some conclusions in Section V.

## II. FRAMEWORK SUMMARY

Three new models (Fig. 1) are used to downscale the aggregate outputs of a national electricity model. These outputs define “boundary conditions” (regional capacity, energy output, and emissions) which are spatially—and temporally—aggregated totals that the downscaling analysis is to disaggregate to particular locations and hours. Boundary conditions for a particular scenario year can be obtained from any national model; here, we use the electricity market model Haiku. Haiku’s structure as well as supply and demand assumptions are documented elsewhere [e.g., [4], [21], [22]], so we only briefly summarize the model here.

Haiku calculates electricity demand, electricity prices, the composition of electricity supply, inter-regional electricity trading activity among 21 regions, and emissions of  $\text{NO}_x$ ,  $\text{SO}_2$ , mercury and  $\text{CO}_2$ . Demand functions and supply curves are calculated for four time periods (super-peak, peak, shoulder, and baseload hours) in each of three seasons (summer, winter, and spring/fall). Hence, 12 market equilibria are identified for each simulation year, in each of 21 linked regions of the country.

Haiku's electricity supply depends on the type of generation technology as well as the cost and characteristics of fuels, and environmental and economic regulations. Generation technology is represented by about 50 categories of generation facilities, distinguished by fuel type and vintage, in each of the 21 model regions. Investment in new capacity and retirements are determined endogenously. The model includes fuel market modules for coal and natural gas, and calculates prices that are responsive to factor demand. Fuel price forecasts are calibrated to match other forecasts including the U.S. EIA Annual Energy Outlook [27]; demand growth assumptions are also consistent with [27]. Demand is modeled as a partial adjustment demand system with elasticities specific to customer class, region, and season. National averages of the short run elasticities are  $-0.11$  to  $-0.16$ , and long run elasticities are three times larger [22].

The first of our three models (EDM1, for "Emissions Downscaling Model 1") allocates Haiku regional capacity to multicounty subregions within states, and simultaneously dispatches that capacity on a detailed temporal basis for an average year. An "average year" is represented by the average load duration curve expected under a given climate. EDM1 considers an aggregated version of the grid, demand locations, fuel price differences, and locations of existing plants.

The second model, EDM2, takes EDM1's new capacity by subregion and allocates new generation facilities in realistic sizes to individual counties. We use an empirical (regression) siting model (one per generation technology) to calculate the probability of siting new facilities in a county as a function of population, non-attainment status (under air pollution laws), and other characteristics. An integer program then assigns capacity to counties in approximate proportion to those probabilities, while respecting the constraint that plants must be realistically sized.

The final model, EDM3, translates the average annual pattern of EDM1 emissions to source-specific hourly emissions for a particular meteorological year. It does this by decomposing the annual average load duration curve (and associated plant operation and emissions) into particular hours within each modeled year. (For instance, within a "2050s" climate scenario, the results of climate simulations may show that one particular year has a large share of peak temperature hours; EDM3 would then assign a proportionate number of the high demand/emissions hours to the high temperature hours of that year.) The result is variation in emissions among years, but averages over the years that are consistent with Haiku regional emissions results.

### III. FORMULATIONS OF EMISSIONS DOWNSCALING MODELS

#### A. EDM1: Subregion Location and Mean Conditions Dispatch

The function of this model is to take the boundary conditions from Haiku for a given power market, distribute new capacity among multicounty subregions in that market, and finally dispatch all capacity to meet an average year's or ozone season's loads, subject to a linearized dc load flow and assumed demand distributions. For instance, in our application in Section IV, we use Haiku energy and emissions for four summer demand periods within an eight state region as boundary conditions, allocate new Haiku capacity among subregions in that region

(e.g., from the Maryland region of Haiku to four subregions within that state), and finally dispatch all the capacity against a more finely-defined load duration curve (here having 16 periods). EDM1's outputs are further disaggregated in space by EDM2 and time by EDM3 (Fig. 1).

Since we assume demands are fixed (based on Haiku's values), we can take advantage of the result that a market equilibrium is equivalent to minimizing cost (e.g., [12]). So we formulate EDM1 as a cost-minimizing linear program (LP):

*Choose the values of the following decision variables:*

- $capn(r, m, i)$ : MW of new generation capacity of each type  $m$  at each node  $i$  in each Haiku region  $r$  in the study region;
- $x_1(k, s, t)$ ,  $x_2(r, m, i, s, t)$ : MW energy produced by existing plant  $k$  and new generation capacity of type  $m$  located at  $(r, i)$ , respectively, in each load period  $p$  and season  $s$ ; and
- $f(i, j, s, t)$ : MW transmission flow from node  $i$  to node  $j$  on a linearized dc network.

*In order to minimize annualized cost, including:*

- operating costs of existing and new capacity, accounting for differentials in fuel, emissions permits, and other costs across subregions; plus
- the annualized capital cost of new generation facilities, when differing across subregions.

*Subject to the following constraints:*

- generation for each generator and time block and season is limited by its capacity, derated for outages;
- boundary conditions that require that appropriate sums of variables across subregions, generators, and model time periods be consistent with Haiku's totals. These can include total generation by each Haiku plant type for each Haiku period; total emissions for each Haiku region and period; and total new generating capacity of each type by Haiku region;
- linearized dc load flow constraints, including energy balances at each node (subregion) in each period and season; flows proportional to voltage angle differences between nodes; losses; and flows limited by transmission capacity; and
- siting constraints that limit where new plants can be put, considering land, water, and fuel transport availability.

The general structure is similar to that used in other regional energy facility location models that have been used for power system planning, geographical downscaling of national energy scenarios, and analyses of environmental and economic regulatory issues [e.g., [9], [11], [14], [20]]. However, EDM1 is unique in including all these features simultaneously.

The basic structure of EDM1 also resembles LP-based capacity expansion models commonly used in the industry [12], [25]. But there are four key differences between EDM1 and such expansion models. These include boundary conditions, siting limitations and costs, and the representation of transmission and loads.

1) *Boundary Conditions:* The most important difference is the boundary conditions. Three types are given below in

(1)–(3): the appropriate sums of disaggregated energy generation, new capacity construction, and emissions are consistent with the Haiku aggregate values:

$$\begin{aligned} & \sum_{k \in k(m), t \in t(s,p)} H(s,t) * x_1(k,s,t) \\ & + \sum_{i \in i(r,m), t \in t(s,p)} H(s,t) * x_2(r,m,i,s,t) \\ & \geq (1 - \theta_{TGEN})TGEN(r,m,s,p) \text{ and} \\ & \leq (1 + \theta_{TGEN})TGEN(r,m,s,p) \\ & \quad \forall r, m \in m(r), s, p \end{aligned} \quad (1)$$

$$\begin{aligned} & \sum_{i \in i(r,m)} capn(r,m,i) = TCAP_2(r,m) \\ & \quad \forall r, m \in m(r) \end{aligned} \quad (2)$$

$$\begin{aligned} & \sum_{k \in k(r), t \in t(s,p)} H(s,t) * E_1(k,s) * x_1(k,s,t) \\ & + \sum_{m \in m(r), i \in i(r,m), t \in t(s,p)} H(s,t) * E_2(r,m,s) \\ & * x_2(r,m,i,s,t) \\ & \geq (1 - \theta_{TNOx})TNOx(r,p) \text{ and} \\ & \leq (1 + \theta_{TNOx})TNOx(r,p) \quad \forall r, s, p. \end{aligned} \quad (3)$$

The index sets we use are defined as follows:

$i(r,m)$	set of nodes $i$ in region $r$ in which new plants of type $m$ can be sited (given availability of land, water, and fuel);
$k(m)$	set of existing generators $k$ that are included in Haiku model plant $m$ . Note that each $k$ is associated with a unique node $i$ ;
$m(r)$	set of Haiku model plants $m$ associated with region $r$ , with each $m$ associated with only one region;
$t(s,p)$	set of time blocks $t$ that are within Haiku period $p = 1, 2, 3, 4$ and season $s \in \{\text{summer, winter, spring/fall}\}$ .

The parameter used are as follows:

$\theta_{TGEN}, \theta_{TNOx}$	relaxation parameters for energy and emissions boundary conditions [dimensionless];
$E_1(k,s)$	$\text{NO}_x$ emission rate of existing plant $k$ [tons/MWh]. Values of $E_1$ and $E_2$ are the same as Haiku data;
$E_2(r,m,s)$	$\text{NO}_x$ emission rate of new plant $(r,m)$ [tons/MWh];
$H(s,t)$	length of EDM1 time block $t$ in season $s$ [hours/yr];
$TNOx(r,p)$	total $\text{NO}_x$ emissions for Haiku region $r$ during Haiku period $p$ [tons/period/yr];
$TCAP_1(k)$	existing capacity of plant $k$ [MW];

$TCAP_2(r,m)$  total capacity of new plant  $(r,m)$  [MW];

$TGEN(r,m,s,p)$  total generation by plant  $(r,m)$  in season  $s$  and Haiku time block  $p$  [MW].

The user has discretion about which of these conditions to enforce. Since our application below is focused on calculating disaggregated emissions, we only impose the new capacity and emissions boundary conditions (2), (3) and omit the energy conditions (1). That is, we site new capacity such that the total new capacity across all subregions in a Haiku region equals the regional total for each type, and dispatch all capacity so that the  $\text{NO}_x$  emissions across all plants in a Haiku region within each Haiku season and period are consistent with the Haiku aggregate value for that region, season and period. However, we allow individual generation totals to differ because transmission losses and flow limits mean that it may not be feasible to exactly match the energy outputs of each plant type.

In our experience, in order to obtain feasible solutions, it has also been necessary to slightly relax the included boundary conditions in some cases. This may indicate that subregional constraints are such that EDM1 yields a more realistic solution than the national model. However, we assume that the purpose of the framework is to disaggregate regional totals, not modify them. Thus we express (1) and (3) as a pair of inequalities that force the downscaled energy and emissions to be within a prespecified range of the Haiku values. When this has been a problem, we have found that values of the parameters  $\theta_{TGEN}, \theta_{TNOx}$  on the order of 1% suffice to yield a feasible downscaling. When applying EDM1, the robustness of the downscaled results to those parameters should be evaluated; ideally, the patterns of emissions would only change insignificantly.

2) *Siting Limitations and Spatially Differentiated Costs:* New power plants of each type can only be built in a subset of locations. For instance, air quality rules prevent use of coal in some areas. Baseload plants use large amounts of cooling water, so they need to be near the coast or large rivers.

The cost of building and operating plants can also vary within a Haiku region. For instance, mine-mouth plants in western Pennsylvania have lower coal costs than plants further east, due to the need for rail transport of coal to the latter. However, Pennsylvania defines a single Haiku region. On average, our downscaling model uses the same variable costs  $C_1$  and  $C_2$  as Haiku, but we differentiate those costs among a Haiku region  $r$ 's subregions  $i$ , increasing them for subregions further from fuel sources and decreasing them for subregions that are closer, based on typical fuel transport costs.

We also differentiate plant construction costs among subregions. Because land is costly in urban areas (such as northern NJ), so construction costs there will be higher. Yet as total new capacity of each type is a fixed boundary condition (2), only differences in capital costs among subregions matter. Thus, the cost of new capacity only has to represent the increment relative to a baseline, instead of the total cost.

3) *Transmission Representation:* We use a linearized dc load flow model, modified to represent quadratic power losses [24]. To preserve the linearity of the model (so we can use efficient LP solvers), the load flow model uses an iterative approach based upon a Taylor's series approximation of the quadratic loss terms

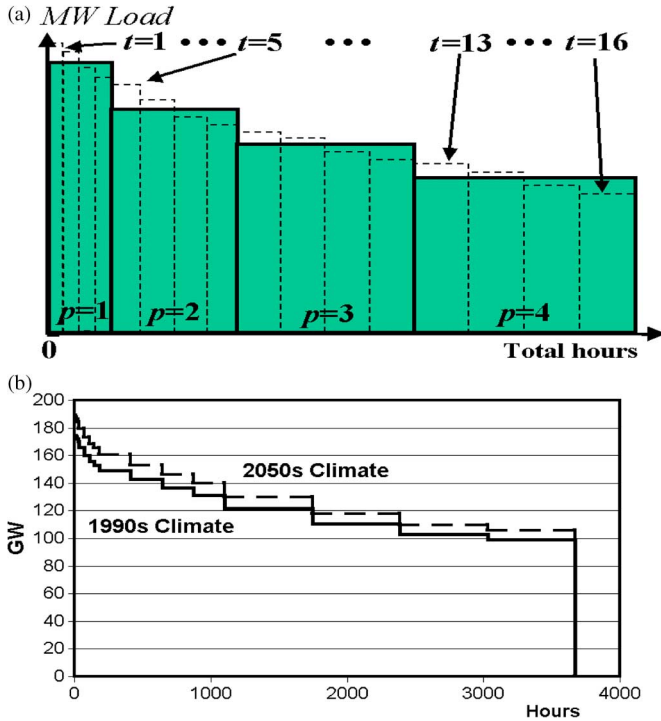


Fig. 2. (a) Schematic of Haiku four-block ( $p = 1, \dots, 4$ ) (solid lines) and EDM1 16-block ( $t = 1, \dots, 16$ ) (dashed lines) approximation of summer load duration curve used in application. (b) Comparison of “1990s Climate” and “2050s Climate” load duration curves for year 2030 market simulations.

[13]. In that approach, an initial solution without any is inserted in a first-order Taylor’s series expression for losses, and a new set of flows obtained by solving EDM1. This process can be repeated until results converge, which occurs within two or three iterations [13]. Alternatively, a nonlinear solver could be used instead of the iterative LP.

We do not represent transmission expansion decisions endogenously, however. This is because expansion of the grid for a linearized dc load flow results in integer variables (for new corridors) and nonlinear expressions for the voltage-flow constraints (since reactance is a function of capacity) [e.g., [19]]. Instead, we use an exogenously specified transmission grid. If instead a transshipment (path-based) formulation of load flow is used, then transmission capacity variables could be included [25], but this would be at the expense of realism of the load flow.

4) *Load Representation*: In order to perform the temporal downscaling, EDM1 has more time blocks than the 12 blocks per year in Haiku. For instance, in the example later in this paper, EDM1 has four time periods  $t$  for each of the four Haiku periods  $p$  during the summer season, or 16 blocks total. Fig. 2(a) compares stylized summer load duration curves implied by the Haiku and EDM1 load representations. Linear models such as Haiku and EDM1 (and LP generation models in general [25]) approximate load duration curves by a series of steps, one per load period with a constant MW load in each period. An interpolation/smoothing procedure is used to define EDM1 blocks whose total energy sum to the Haiku energy in each associated  $p$  while providing a better approximation of the underlying smooth load duration curve. Fig. 2(b) shows the resulting curves

for our 2030 market simulation under the two climate scenarios used in the case study of Section IV.

The load duration curves in Haiku and EDM1 represent expected annual load duration curves, averaged over the possible yearly load distributions that vary from year to year because of meteorology. As Section III-C explains, hourly time profiles of emissions for particular years are derived by EDM3 from the average output of EDM1 by associating particular hours in each meteorological year with the EDM1 load blocks.

Since air quality models need specific facility locations, we could have formulated EDM1 as a mixed integer program that sites realistically sized plants at a finer scale. However, such a model is more difficult to solve, and would assume that all siting considerations can be captured in a cost function. Instead, we developed EDM2 to capture empirical patterns of siting while disaggregating EDM1 results to the county level.

### B. EDM2: County-Level Siting of New Capacity

These models allocate new subregional capacity  $cap_m(m, r, i)$  to the county level in reasonably sized generation units. This allocation is done in two steps in EDM2. First, we calculate the expected probability of siting of each particular plant type in each county based on the county’s characteristics. Then an optimization model attempts to allocate plants as consistently as possible with those probabilities, as gauged by a squared deviations objective. The regression models used by EDM2 are described in detail elsewhere [5]. In essence, the probability  $p(m, c)$  of siting one or more new generation units type  $m$  in county  $c$  is estimated as a function of independent variables  $Y = \{y(n, c), n = 1, 2, \dots\}$  using a log logit formulation:

$$\log [p(m, c) / (1 - p(m, c))] = a(m) + \sum_n b(m, n) y(n, c) \quad (4)$$

where  $a(m)$  and  $b(m, n)$  are estimated coefficients. This standard transformation takes any variable that is confined to the range (0,1) (such as probability) and converts it to a variable on the real line [8], thereby ensuring that any calculated  $p(m, c)$  will be in that range. Future research could test nonlinear relationships, such as saturation effects, in which the presence of capacity increases the probability only up to a point.

The values of the coefficients are estimated using a maximum likelihood method from historical siting decisions in the period 1995–2004, using all continental U.S. counties as the database. The independent variables include presence of existing generators, ozone attainment status, population variables, state utility deregulation status, and median income. The equation is estimated separately for  $m = \text{coal-fired baseload plants, combined cycle plants, and combustion turbines}$ .

Given the estimated coefficients, the values of  $p(m, c)$  are calculated using (4) for each county  $c$  in the region modeled. Sample values are provided in Section IV-C, below. The next step is to use those probabilities to allocate new capacity  $cap_m(m, r, i)$  in subregion  $i$  to counties  $c \in c(i, m)$ , where  $c(i, m)$  is the set of counties in subregion  $i$  in which plants of type  $m$  can be sited. EDM2 does this by trying to distribute capacity to counties in proportion to their  $p(m, c)$ , while respecting the constraint that only integer numbers of units can be sited.

The formulation is presented after defining notation:

$U(m)$	standard generating unit size for generating unit type $m$ , in MW (e.g., coal steam = 600 MW);
$capn'(m, r, i) = capn(m, r, i) - [capn(m, r, i) \text{ MOD } U(m)]$	(i.e., the capacity of the largest integer number of generating units whose capacity is no more than $capn(m, r, i)$ );
$N(m, r, i) = capn'(m, r, i) / U(m)$	
$ns(m, c)$	number of generating units of type $m$ sited in county $c$ ;
$p'(m, c) = p(m, c) / \sum_{c \in c(i, m)} p(m, c)$	for each subregion $i$ , the rescaled probability for county $c$ and plant type $m$ .

The model is then as follows:

$$\text{MIN } \sum_{c \in c(i, m)} [ns(m, c) - p'(m, c)N(m, r, i)]^2 \quad (5)$$

Subject to :

All plants are sited :

$$\sum_{c \in c(i, m)} ns(m, c) = N(m, r, i) \quad (6)$$

Only integer numbers of plants are sited :

$$ns(m, c) \in \{0, 1, 2, \dots\} \quad \forall c \in c(i, m). \quad (7)$$

A challenge in solving (5)–(7) is that it the model is a non-linear integer program, which can be hard to solve to optimality. Heuristic methods that yield good but not necessarily optimal solutions can also be applied.

The resulting solution is then translated into the amount of new capacity  $capn_{co}(m, c)$  of type  $m$  in each county  $c$  as follows.

For each subregion  $i$ :

$$\begin{aligned} capn_{co}(m, c) &= ns(m, c)U(m) + [capn(m, r, ic(c)) \text{ MOD } U(m)] \\ &\text{for } c \in c(i, m) \text{ having the highest } p'(m, c) \text{ in that subregion} \\ capn_{co}(m, c) &= ns(m, c)U(m) \text{ for all other } c \in c(i, m) \end{aligned}$$

In words,  $ns(m, c)$  generating units of size  $U(m)$  are assigned to county  $c$ . The only exception is the county with the highest probability, which is also allocated the remainder capacity that cannot be assigned as an integer unit. For the purposes of air quality simulations, all new capacity in a county  $c$  is assumed to be sited at its geographic centroid.

Geographic downscaling of emissions can then be completed by taking EDM1's total emissions for a subregion  $i$ 's capacity of type  $m$  for each period, and dividing it among the existing and new generators of that type in proportion to their capacity in  $i$ , while accounting for meteorology. This is described next.

### C. EDM3: Allocation of Emissions to Hours

However, to perform an air quality simulation, further temporal downscaling is required. In particular, emissions must be specified on an hourly basis, consistent with the chronology of temperatures and other meteorological variables. For instance, higher air conditioning loads and, thus, higher  $\text{NO}_x$  emissions is associated with hotter and stiller meteorology that, in an unhappy coincidence, also increases the likelihood of smog episodes. Thus, the probability of extreme pollution concentrations increases compared to the naïve assumptions that power plant emission rates are unaffected by weather (as assumed, e.g., in SMOKE [28]) or vary independently of weather. If climate warming occurs, it would increase the frequency of hot days, running the risk of increased frequency of ozone episodes, even if seasonal or annual  $\text{NO}_x$  emissions are capped.

Therefore, we developed EDM3 to distribute the average annual emissions resulting from EDM1 among hours in particular years consistent with the meteorology in those years. The assumption is that the annual load duration curve used in EDM1 (Fig. 2) can be viewed as being assembled from the actual load duration curves of a sample of years by ordering all hourly loads from all years from most to least MW, and then rescaling the hours axis. To allocate emissions to individual years, we reverse this assembly process after solving EDM1; this reversal simply notes the specific hours of each year that occur in each of EDM1's load blocks  $t$  in Fig. 2, and then assigns the EDM1 emissions to those hours. So, for instance, if "2055" is a particularly hot year in the "2050s" scenario, then it will have more hours occurring in the peak block (far left of Fig. 2) than, say, "2054" if the latter is a relatively cool year. The "2054" peak block loads might occur (say) between 16:00 and 19:00 on July 23, so the EDM1 emission rates for the peak block would be assigned to those hours.

The EDM3 procedure follows the below three steps, yielding an hourly time series of emissions for each power plant.

- Step 1) For a sample of  $Y$  years (for instance a decade), obtain hourly temperature data for a selection of weather stations in the region being modeled. The data could be from historical records, or could be generated by climate simulation models. In our application, we use the MM5 module to down-scale multiyear climate scenarios generated by the GISS global circulation model (as in [15], [33]). We accessed GISS simulations for two different "climates": a "1990s" climate, representing average climate conditions in that decade, and a "2050s" climate, representing conditions under a doubling of atmospheric  $\text{CO}_2$  concentrations. Note that these data are simulations, and not actual observations. We compare the distributions of emissions resulting from those two decades in Section IV.
- Step 2) Develop a statistical short-run load forecasting model that projects hourly load for a given subregion or collection of subregions based on historical

data. For the application below, we used a simple model specification that is quadratic in temperature and uses dummy variables for day of the week and hour of the day:

$$L(i, y, h) = A_L + B_{T1}(i, y, h)T(i, y, h) + B_{T2}(i, y, h)T(i, y, h)^2 + B_W D_W(y, h) + \sum_{h'=2, \dots, 24} B_{h'} D_h(h, h') \quad (8)$$

where:

$L(i, y, h)$  load in subregion  $i$  in hour  $h$  of year  $y$  [MW];

$T(i, y, h)$  temperature in subregion  $i$  in hour  $h$  of year  $y$  [ $^{\circ}$ C];

$D_W(y, h)$  dummy variable, indicating whether the hour occurs during a weekday (1) or weekend (0);

$D_h(h, h')$  dummy variable, with a 1 indicating that the hour  $h$  is associated with hour  $h' \in \{2, \dots, 24\}$ . (The dummy is zero for the first hour  $h' = 1$ .);

$A_L, B_{T1}, B_{T2}, B_W, B_{h'}$  regression coefficients, which are specific to the subregion whose loads are modeled.

Other more sophisticated time series, neural network, or other models can instead be used (as in [5]), as long as the input variables are available from the meteorological simulation.

- Step 3) For all hours  $h = 1, 2, \dots, H$ , in all years  $y$  in the time period under consideration (e.g., the “2050s”), rank the hours in decreasing order according to the total estimated regional load  $\sum_i L(i, y, h)$ , with the rank of the  $h$ th hour being  $R_h(h)$ . (For instance, if  $Y = 10$  years, then there would be  $H = 87600$  hours, ignoring Feb. 29 in leap years. If  $h = 10367$  is the highest load hour, then  $R_h(10367) = 1$ . In that case, if  $h = 23998$  is the lowest load hour, then  $R_h(23998) = 87600$ .) With  $T$  being the total number of time blocks in EDM1, let  $R_t(t, s)$  be cumulative number of hours of all load blocks that have a load equal or exceeding load block  $t$  in season  $s$ . [E.g., if  $t = 1, s = \text{summer}$  and  $t = 2, s = \text{summer}$  have the first and second highest loads, respectively, and each lasts 16 hours per year and  $Y = 10$  years, then  $R_t(1, \text{summer}) = 160$  and  $R_t(2, \text{summer}) = 320$ .] Let  $\underline{X}_{EDM1}(t, s) = \{x_1(k, s, t), x_2(r, m, i, s, t), \forall r, m, i, k\}$  be the vector of EDM1 generation variables for season  $s$  and period  $t$ . Finally, let  $\{t(h), s(h)\}$  be the value

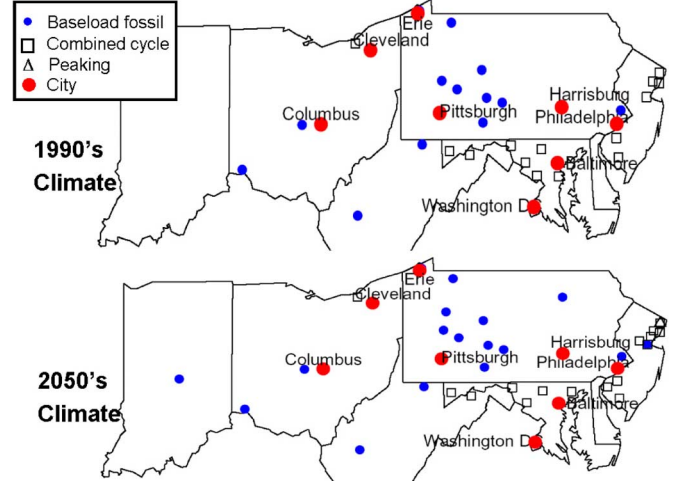


Fig. 3. Study region for downscaling, along with EDM2 siting results for 2030 under two climate scenarios.

of the vector  $\{t, s\}$  in which hour  $h$  occurs; i.e., this is the value of  $\{t, s\}$  such that  $R_t(t, s)$  is the lowest possible value that still exceeds  $R_h(h)$ . Then dispatch  $\underline{X}_{EDM1}(t(h), s(h))$  and its associated emissions are assigned to hour  $h$ . This assignment is repeated for all  $h$  in the years of interest. The resulting hourly series of geographically disaggregated emissions would then be used in the air quality model by assuming that all plants of a given type  $m$  in a given subregion  $i$  have the same emissions rate per MW of capacity.

An important assumption in EDM3’s procedure for allocating emissions among years is that banking of  $\text{NO}_x$  allowances is allowed (as it is under present U.S. law), and that generators have perfect knowledge of the price of and need for allowances. In particular, we assume that emissions can be shifted from low demand years to high demand years such that the price of allowances is the same in all years.

#### IV. APPLYING THE FRAMEWORK: PJM-ECAR 2030 UNDER TWO DIFFERENT CLIMATES

The downscaling modeling framework EDM1-EDM3 has been implemented for the eight states shown in Fig. 3. This region includes the original PJM market plus the coal generating states of Ohio and Indiana, which we call the “PJM-ECAR” region. We illustrate the use of our framework by downscaling year 2030 emissions from two Haiku market solutions: one under a “present climate” scenario (“1990s”) and the other under an accelerated warming scenario representing a doubling of  $\text{CO}_2$  concentrations (“2050s”).

##### A. Assumptions

We simulate power markets for the year 2030 because it is the last year considered by Haiku. We consider the extreme cases of no climate change (“1990s climate”) and a doubling of  $\text{CO}_2$  (“2050s climate”) to show how climate can affect the results. In the “1990s” Haiku solution, all demand and fuel price assumptions are consistent with USEIA [27] projections. However, in the “2050s” scenario, heating- and cooling-degree days in the United States are assumed to change in a linear fashion

over the Haiku solution years (2005, 2010, etc.) until 2030, at which time they are assumed to be consistent with the average values calculated from the GISS “2050s” scenario. For instance, the “1990s” average summer temperature of 72.9°F in Pennsylvania would, under the GISS scenario, warm to 75.5°F by 2030. Summer warming varies from 1.5 to 2.5°F among the states in the study region, while winter warming is approximately twice as much.

This warming affects electricity consumption (through Haiku’s demand functions which depend on heating- and cooling-degree days) and thus electricity prices and capacity. Haiku projects that overall U.S. energy generation and prices in 2030 are a total of 2% higher, on average, in the warming scenario (“2050s climate”) relative to the unchanged climate scenario (“1990s climate”), while capacity increases by 8% to accommodate summer peaks. Fig. 2(b) shows the summer load duration curve for the Haiku regions including the PJM-ECAR study region, revealing the higher demands under the “2050s” climate. No national CO<sub>2</sub> legislation is assumed to be in place (consistent with USEIA [27] assumptions), so CO<sub>2</sub> emissions increase under the warmer climate. But regional SO<sub>2</sub> and NO<sub>x</sub> caps mean that annual emissions of those pollutants in the eastern U.S. change little, although their timing can change because of shifts in demand patterns. The stress that higher temperatures place on markets is evidenced by higher NO<sub>x</sub> prices; the 2030 summer NO<sub>x</sub> price is almost three times higher in the “2050s” scenario than in the “1990s” scenario.

Haiku results for the two scenarios are downscaled to the eight state region in Fig. 3 using a version of EDM1 that provides considerable detail on the summer ozone season (May–September). A total of 500 Haiku model plants  $m$  are considered, representing 3719 individual existing plants  $k$  as well as new capacity. Each Haiku summer load block  $p$  [Fig. 2(b)] is divided into four EDM1 load blocks  $t$ , for a total of 16 summer blocks with the following number of hours in each:

$$\begin{aligned} t=1-4 &: 9 \text{ hours/block}; & t=5-8 &: 37 \text{ hours/block}; \\ t=9-12 &: 229 \text{ hours/block}; & t=12-16 &: 643 \text{ hours/block} \end{aligned}$$

The total number of summer hours are 3672 hours. Thus, we provide more detail for the peak blocks when emissions (and their impacts, due to hot weather) are likely to be highest.

Our approximation of the transmission network in the eastern part of the study region is shown in Fig. 4.

### B. EDM1 Results: Average NO<sub>x</sub> Emissions Distributions

Fig. 5 shows emissions duration curves that result from EDM1 for the summer ozone season in the eight states based on the average load duration curves for 2030 [Fig. 2(b)]. One curve is shown for each climate scenario. The total emissions under each curve is equal, consistent with the assumption of a cap-and-trade policy. However, the distributions within the season differ, especially during the peak, when the 2050s climate yields higher peak emissions (by about 3%). This may understate the actual increase that would result from climate warming, since Haiku’s present demand model does not change the within-season load shape, even though more air conditioning would take place. (Other energy models can account for load shape changes due to changes in mixes of

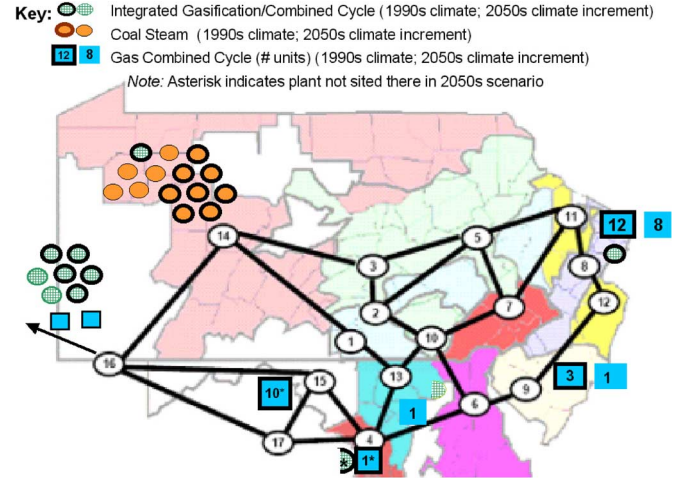


Fig. 4. Assumed transmission grid and EDM1 allocation of new Haiku capacity among subregions (OH, IN, WV, and SW PA capacity shown together).

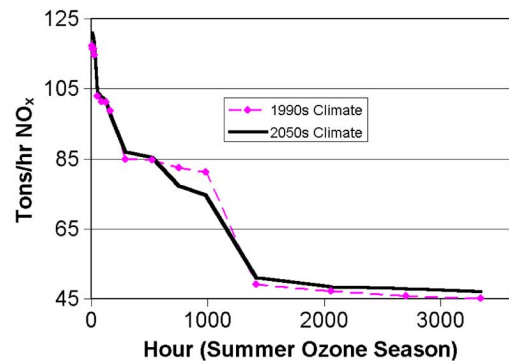


Fig. 5. Mean 2030 NO<sub>x</sub> emissions duration curves from EDM1 for study region for “1990s” and “2050s” climate scenarios.

energy-using equipment, such as NEMS [27], which was used in the downscaling study by Chen *et al.* [5].)

But to judge whether these differences are significant, we need to consider the variation of curves from year to year within a climate scenario. We do this in Section IV-D, below.

It is possible that a greater concentration of emissions into certain hours under the “2050s” scenario could provoke a reaction by local authorities. Yet, consistent with the philosophy of national energy models, e.g., NEMS, we take as given the present national and state regulatory structure. It would be interesting to postulate changes in local rules in response to shifts in emissions locations or timing. However, endogenizing rules would involve making arbitrary assumptions about future political attitudes and their translation into rule changes; this would introduce complexity and reduce model transparency.

Fig. 4 shows how EDM1 distributes the new generation capacity created by Haiku by the year 2030 in response to demand growth. Individual 600 MW baseload units are shown as separate circles, while a single square indicates a region where combined cycle capacity is sited (with the number of 400-MW units being indicated within the square). (Not shown in the figure is the modest amount of combustion turbine capacity that is also sited in northern NJ.) These additions are over and above those that have already been announced by generation companies. The figure reveals that baseload coal plants dominate in

TABLE I  
MODEL EDM2 INPUT: COUNTIES WITH LARGEST AND SMALLEST PROBABILITIES OF NEW PLANT SITING BY STATE

State	Min or Max <sup>a</sup>	County (Baseload Plant Probability)	County (Combined Cycle Probability)
DE	Min	Sussex (.26)	Sussex (.09)
	Max	New Castle (.43)	Kent (.42)
IN	Min	Tipton (.06)	Orange (.01)
	Max	Marion (.54)	Allen (.18)
MD/DC	Min	Queen Anne (.12)	Baltimore City (.04)
	Max	Anne Arundel (.54)	Montgomery (.77)
NJ	Min	Sussex (.16)	Passaic (.10)
	Max	Middlesex (.57)	Hunterdon (.48)
OH	Min	Union (.13)	Athens (.04)
	Max	Hamilton (.69)	Cuyahoga (.64)
PA	Min	Cameron (.14)	Cameron (.05)
	Max	Montgomery (.57)	Montgomery (.51)
WV	Min	Morgan (.06)	McDowell (.01)
	Max	Monongalia (.21)	Grant (.05)

<sup>a</sup>For baseload plants, these exclude counties with high population density or inadequate water supplies where such plants are unlikely to be sited.

mid- and northwest PA, while integrated gasification-combined cycle facilities are more important further west. Gas-fired combined cycle plants are the major type of new plant sited in the east. The figure shows “1990s” climate additions in circles or squares with a black border; in most cases, the “2050s” climate adds that capacity plus the additional capacity shown in circles or squares without a border. Thus, the “2050s” climate has more baseload capacity in the west, and eight more combined cycle units in northern NJ.

C. EDM2 Results: Siting Scenarios by County

The regression models (4) used by EDM2 show the probability by county of siting baseload, combined cycle, and peaking power plants, based on historical siting patterns. The range of results for each state is shown in Table I. For instance, Montgomery County, PA has about four times the probability of hosting a new baseload power plant as Cameron County, PA.

The results of solving the integer programming problem (5)–(7) with a heuristic are shown in Fig. 3, above. The new plants whose location by subarea are shown in Fig. 4 are allocated to counties in Fig. 3 with the highest siting probabilities within each subarea. Consistent with historical patterns, baseload plants are sited mainly in the coal-bearing areas, while combined cycle and peaking units are located closer to load centers in the NJ-MD urban corridor.

D. EDM3 Results: Chronologic Hourly Emissions Scenarios

EDM1 produces average annual emissions duration curves for individual generating facility classes *m* by subregion; EDM3 disaggregates those curves to produce hourly sequences for particular years of emissions by generating facility that can then be used in air quality simulations.

For instance, Fig. 6 shows the total regional emissions profiles for two relatively hot weeks based on the 2030 Haiku results, one from the “1990s” climate (end of July in GISS simulation year “1997”) and one from the “2050s” climate (end of July in GISS simulation year “2055”). The average temperatures are shown below the emissions, illustrating the strong relationship between the two. For instance, the first day in the 1990s week

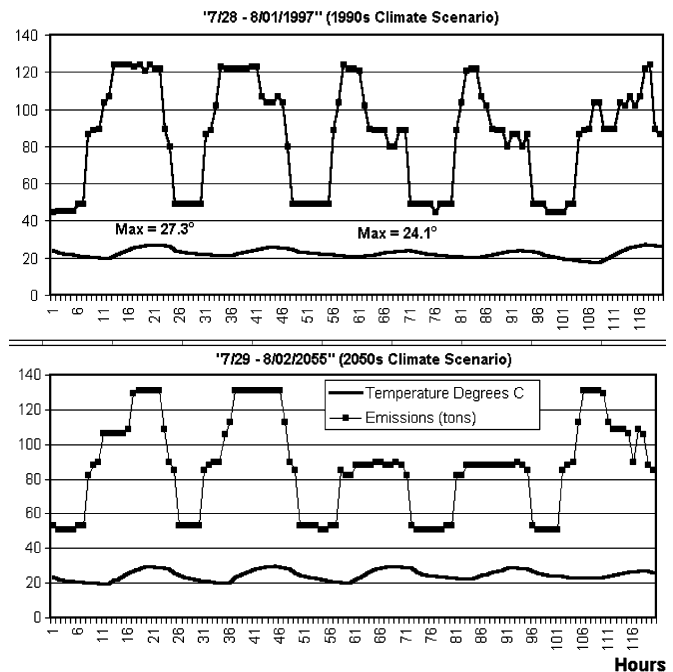


Fig. 6. Two weeks of NO<sub>x</sub> emissions from “1990s” and “2050s” scenarios.

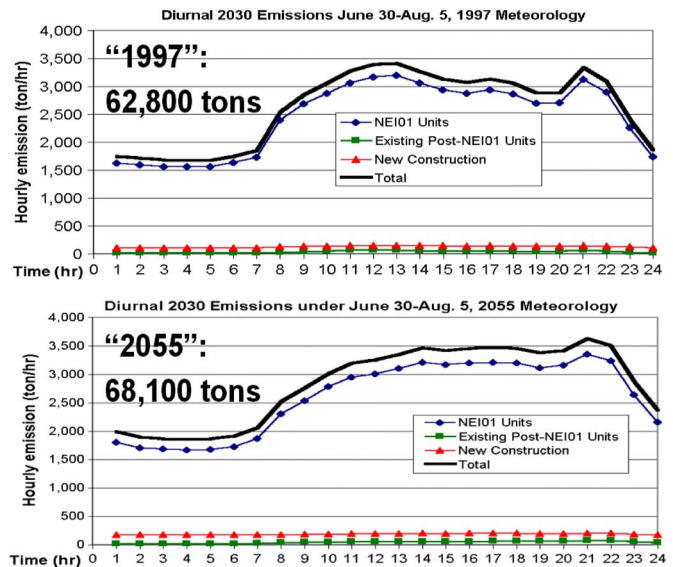


Fig. 7. Diurnal NO<sub>x</sub> emissions patterns for two five-week periods.

has a peak temperature of 27.3°C, and has higher emissions than the third day, whose peak temperature is only 24.1°C. The week from the 2050s climate is an example of an even stronger variation in emissions among weekdays.

Consistent with Fig. 5, Fig. 6 shows that peak emissions from the 2050s climate are approximately 10 tons/hour higher than the peak emissions for the 1990s climate as a result of the higher peak demands under the former climate. This occurs even though total NO<sub>x</sub> during the ozone season (averaged over the years within the scenario) must be the same due to the cap-and-trade system.

Fig. 7 shows the average diurnal emissions pattern for the days comprising a five week period in each of the two climate scenarios based upon EDM3’s processing of the 2030

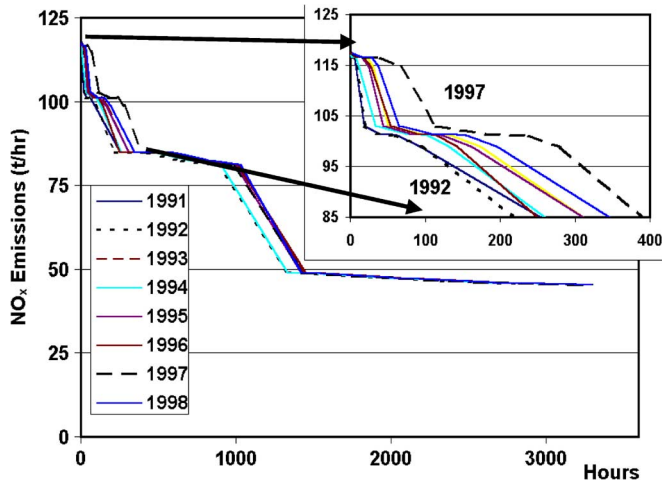


Fig. 8. Regional  $\text{NO}_x$  emissions duration curves based on 2030 market conditions for individual years in “1990s” climate scenario.

Haiku projections. The “2055” climate results shows higher total emissions, despite the same cap being imposed in both climate scenarios, perhaps because this is a hotter than average year for the “2050s” scenario, and also because the emissions pattern is “peakier” under a warmer climate (consistent with Fig. 5). The figure also shows the breakdown in emissions between plants that were built by 1999 (the NEI01 units that are in USEPA’s inventory for 2001 [30]), newer actual plants, and Haiku-created capacity. By far, most emissions are from existing facilities, since new plants must comply with stringent New Source Performance Standards. This is so even in 2030 and in spite of Haiku assuming much tighter emissions caps than are in place today. (Haiku’s regulatory assumptions are consistent with USEPA’s Clean Air Interstate Rule.)

From each year’s hourly emissions, we can assemble emissions duration curves for each year and compare them to assess the effect of year-to-year meteorological variability on emissions. Fig. 8 shows a comparison of eight years of  $\text{NO}_x$  emissions under the “1990s” climate scenario (again, consistent with the 2030 Haiku projections). We enlarge the peak emissions, which, unfortunately, are most likely to occur during hot days in ozone episodes. The curves show that “1997” (a relatively hot year in the GISS simulations of the “1990s” climate) has appreciably higher peak emissions than “1992” (a cool year). The difference is about 10%. However, total emissions during the ozone season (the integrals of the duration curves) do not vary as much among years.

The 10% range in peak emissions among years in a scenario is greater than the difference between average peak emissions in the “1990s” and “2050s” scenarios shown in Fig. 5. This suggests that year-to-year variability in weather could impact peak emissions more than climate warming. However, more analysis is needed to confirm that conclusion. This is because it depends critically on the effect of climate warming upon demand patterns within the day, which, as mentioned above, may change in ways not presently captured by Haiku’s demand models. Chen *et al.* [5], using a different national model (NEMS) and a different downscaling technique, found more of an impact of climate on average emission patterns.

## V. CONCLUSION

In downscaling future emissions scenarios, it is important to remember that models of economic response to climate change “are for insights not numbers” [23] and that “it’s tough to make predictions, especially about the future” (attributed to Yogi Berra). The purpose of our downscaling framework is *not* to make specific forecasts about plant siting or environmental impacts at particular locations. This is because of large uncertainties in future policy, technology, economic, and environmental conditions, and because particular decisions of particular market participants cannot be predicted.

Rather, the intent is to develop scenarios of emissions that are consistent with market mechanisms for planning and dispatch, and both average and hour-to-hour weather patterns. The use of optimization to determine least cost operations and plant siting subject to environmental and technical constraints is consistent with the operation of competitive markets. The generation of hourly emissions patterns consistent with both general climate trends and hourly weather is important to capture the correlation between high emissions rates and conditions favorable to smog formation. This is accomplished by using scenarios from national energy models that represent the effects of climate upon generation mix and emissions, as well as hourly meteorological simulations to generate hourly demand patterns, power generation, and emissions.

Detailed air quality modeling requires hourly emissions for particular stacks, and we have demonstrated how an optimization-based downscaling method can provide that information. Our downscaling framework is most useful for comparing broadly different scenarios, and provides a logically consistent approach to deducing the implications of different assumptions upon the general effects on the spatial and temporal pattern of pollution. To the extent that future conditions deviate from those assumed, particular quantitative conclusions are uncertain. Nonetheless, the framework can be used to explore how robust qualitative conclusions (such as the peakier emissions projected for a warmer climate) are to changed assumptions.

Future research should apply this framework to address how alternative technology and economic trends could affect the power sector’s environmental impacts. It is also desirable to validate the model by evaluating how well the framework would have predicted the patterns of power generation development in the recent past.

## REFERENCES

- [1] A. D. Amato, M. Ruth, P. Kirshen, and J. Horwitz, “Regional energy demand responses to climate change: Methodology and application to the Commonwealth of Massachusetts,” *Climatic Change*, vol. 71, pp. 175–201, 2005.
- [2] M. L. Bell, R. Goldberg, C. Hogrefe, P. L. Kinney, K. Knowlton, B. Lynn, J. Rosenthal, C. Rosenzweig, and J. A. Patz, “Climate change, ambient ozone, and health in 50 US cities,” *Climatic Change*, vol. 82, pp. 61–76, 2007.
- [3] L. G. Berry, D. J. Bjornstad, and F. D. Boercker, National Coal Utilization Assessment: A Preliminary Assessment of Coal Utilization in the South, Oak Ridge Nat. Lab., Oak Ridge, TN, ORNL/TM-6122, 1978.
- [4] D. Burtraw, K. Palmer, R. Bharvirkar, and A. Paul, “Cost-effective reduction of  $\text{NO}_x$  emissions from electricity generation,” *J. Air & Waste Manage.*, vol. 51, pp. 1476–1489, 2001.
- [5] Y. Chen, B. F. Hobbs, J. H. Ellis, C. Crowley, and F. Joutz, Impacts of Climate Change on Power Sector  $\text{NO}_x$  Emissions: A Long Run Analysis of the Mid-Atlantic Region, University of California-Merced, 2008.

- [6] R. L. Church and T. L. Bell, "A comparison of two baseline screening approaches to regional energy facility siting," *GeoJournal*, no. Supplementary Issue 3, pp. 17–36, 1981.
- [7] J. L. Cohon, C. S. ReVelle, J. Current, T. Eagles, R. Eberhart, and R. Church, "Application of a multiobjective facility location model to power plant siting in a six-state region of the U.S.," *Comput. & Oper. Res.*, vol. 7, pp. 107–123, 1980.
- [8] C. Dougherty, *Introduction to Econometrics*, 3rd ed. London, U.K.: Oxford Univ. Press, 2002.
- [9] W. R. Emanuel, B. D. Murphy, and D. D. Huff, "Optimal siting of energy facilities for minimum air pollutant exposure on a regional scale," *J. Environ. Manage.*, vol. 7, no. 2, pp. 147–155, 1978.
- [10] S. W. Hadley, D. J. Erickson, J. L. Hernandez, C. T. Broniak, and T. J. Blasing, "Responses of energy use to climate change: A climate modeling study," *Geophys. Res. Lett.*, vol. 33, no. 17, p. L17703, 2006.
- [11] B. F. Hobbs, "Regional energy facility location models for power system planning and policy analysis," in *Analytic Techniques for Energy Planning*, B. Lev, F. Murphy, J. Bloom, and A. Gleit, Eds. Amsterdam, The Netherlands: North-Holland, 1984, pp. 53–66.
- [12] B. F. Hobbs, "Optimization methods for electric utility resource planning," *Eur. J. Oper. Res.*, vol. 83, no. 1, pp. 1–20, May 1995.
- [13] B. F. Hobbs, G. Drayton, E. B. Fisher, and W. Lise, "Improved transmission representations in oligopolistic market models: Quadratic losses, phase shifters, and DC Lines," *IEEE Trans. Power Syst.*, vol. 25, no. 3, pp. 1018–1029, Aug. 2008.
- [14] B. F. Hobbs and P. M. Meier, "An analysis of water resources constraints on power plant siting in the mid-Atlantic states," *Water Resources Bull.*, vol. 15, no. 6, pp. 1666–1676, 1982.
- [15] C. Hogrefe, J. Biswas, B. Lynn, K. Civerolo, J.-Y. Ku, J. Rosenthal, C. Rosenzweig, R. Goldberg, and P. L. Kinney, "Simulating regional-scale ozone climatology over the eastern United States: Model evaluation results," *Atmo. Environ.*, vol. 38, no. 17, pp. 2627–2638, 2004.
- [16] C. Hogrefe, C. Rosenzweig, P. Kinney, J. Rosenthal, K. Knowlton, B. Lynn, J. Patz, and M. Bell, "Health impacts from climate-change induced changes in ozone levels in 85 United States cities," *Epidemiology*, vol. 15, no. 4, pp. S94–S95, 2004.
- [17] J. L. Levy, S. L. Greco, and J. D. Spengler, "The importance of population susceptibility for air pollution risk assessment: A case study of power plants near Washington, DC," *Environ. Health Persp.*, vol. 110, no. 12, pp. 1253–1260, 2002.
- [18] D. L. Mauzerall, B. Sultan, J. Kim, and D. Bradford, "NO<sub>x</sub> emissions: Variability in ozone production, resulting health damages and economic costs," *Atmo. Environ.*, vol. 39, pp. 2851–2866, 2005.
- [19] S. A. McCusker, B. F. Hobbs, and Y. Ji, "Distributed utility planning using probabilistic production costing and generalized Benders decomposition," *IEEE Trans. Power Syst.*, vol. 17, no. 2, pp. 497–505, May 2002.
- [20] P. M. Meier, "Energy modeling in practice: An application of spatial programming," *OMEGA*, vol. 10, no. 5, pp. 483–491, 1982.
- [21] A. Paul, E. Myers, and K. Palmer, A Partial Adjustment Model of U.S. Electricity Demand by Region, Season, and Sector Resources for the Future, RFF DP 08-50, 2008.
- [22] A. Paul, D. Burtraw, and K. L. Palmer, The RFF Haiku Electricity Market Model, Resources for the Future report, Washington, DC, 2009.
- [23] J. Peace and J. Weyant, Insights Not Numbers: The Appropriate Use of Economic Models, Pew Center on Global Climate Change, Apr. 2008.
- [24] F. C. Schweppe, M. C. Caramanis, R. E. Tabors, and R. E. Bohn, *Spot Pricing of Electricity*. Norwell, MA: Kluwer, 1988.
- [25] R. Turvey and D. Anderson, *Electricity Economics: Essays and Case Studies*. Baltimore, MD: Johns Hopkins Univ. Press, 1977.
- [26] U.S. Climate Change Science Program, Effects of Climate Change on Energy Production and Use in the United States, Synthesis and Assessment Product 4.5, Oct. 2007.
- [27] USEIA, Annual Energy Outlook 2007, DOE/EIA-0383(2007), 2007.
- [28] USEPA, Science Algorithms of the EPA Models-3 Community Multiscale Air Quality (CMAQ) Modeling System, EPA/600/R-99/030, 1999.
- [29] USEPA, EPA Modeling Applications Using the Integrated Planning Model 2008. [Online]. Available: <http://www.epa.gov/airmarkets/epa-ipm/>.
- [30] USEPA, National Emissions Inventory Air Pollutant Emissions Trends Data 2008. [Online]. Available: <http://www.epa.gov/ttn/chieftrends/index.html>.
- [31] T. D. Veselka, A. Botterud, G. Conzelmann, V. Koritarov, L. A. Poch, and J. Wang, Climate Change Impacts on the Electric Power System in the Western United States, Argonne Nat. Lab., Dec. 2007.
- [32] F. M. Vukovich, R. Wayland, and J. Sherwell, "Characteristics of ozone in the Baltimore-Washington area as established from one-hour average concentrations," *J. Air & Waste Manage. Assoc.*, vol. 49, pp. 794–803, 1999.
- [33] S. Wu, L. J. Mickley, E. M. Leibensperger, D. J. Jacob, D. Rind, and D. G. Streets, "Effects of 2000–2050 global change on ozone air quality in the United States," *J. Geophys. Res.*, vol. 113, p. D18312, 2008.

**Benjamin F. Hobbs** (F'08) is the Theodore K. and Kay W. Schad Professor of Environmental Management in the Department of Geography and Environmental Engineering (DoGEE) of The Johns Hopkins University (JHU), Baltimore, MD.

**Ming-Che Hu** received the Ph.D. degree from the Department of Geography and Environmental Engineering (DoGEE) of The Johns Hopkins University (JHU), Baltimore, MD.

He is a Postdoctoral Researcher in the Energy Bioscience Institute and Department of Agricultural and Biological Engineering at University of Illinois at Urbana-Champaign.

**Yihsu Chen** (A'06–M'07) received the M.S. degree in public health from Harvard University, Cambridge, MA, in 1999 and the Ph.D. degree from the Department of Geography and Environmental Engineering (DoGEE) of The Johns Hopkins University (JHU), Baltimore, MD.

He is an Assistant Professor in the University of California, Merced.

**J. Hugh Ellis** received the Ph.D. degree in civil engineering from the University of Waterloo, Waterloo, ON, Canada, in 1984.

He is a Professor of environmental systems in the Department of Geography and Environmental Engineering at the Johns Hopkins University, Baltimore, MD. He chairs the Department of Civil Engineering and is jointly appointed in the Department of Environmental Health Sciences.

**Anthony Paul** received the M.S. degree in economics from the University of Wisconsin, Madison.

He is the Electricity and Environment Program Fellow at Resources for the Future, Washington, DC.

**Dallas Burtraw** received the Ph.D. degree in economics from the University of Michigan, Ann Arbor.

He is a Senior Fellow at Resources for the Future, Washington, DC.

**Karen L. Palmer** received the Ph.D. degree from Boston College, Boston, MA, in 1990.

She is the Darius Gaskins Senior Fellow at Resources for the Future, Washington, DC.